Quasilinear evolution of the weakly relativistic electron cyclotron maser instability

L. F. Ziebell

Citation: Physics of Plasmas **4**, 2697 (1997); doi: 10.1063/1.872139
View online: http://dx.doi.org/10.1063/1.872139
View Table of Contents: http://scitation.aip.org/content/aip/journal/pop/4/7?ver=pdfcov
Published by the AIP Publishing

Quasilinear evolution of the weakly relativistic electron cyclotron maser instability

L. F. Ziebell[a)]
Instituto de Física, Universidade Federal do Rio Grande do Sul, Caixa Postal 15051, 91501-970 Porto Alegre, RS, Brasil

(Received 2 January 1997; accepted 16 April 1997)

This paper presents a quasilinear analysis of the relativistic electron cyclotron maser instability in which the self-consistent set of equations governing the evolution of the particle distribution function and the energy spectra of unstable waves is numerically solved for parameters typical of the Earth's auroral zone plasma, taking into account both resonant and non-resonant diffusions. The results obtained show that only $0.1\% \sim 0.2\%$ of the particle energy is converted into wave energy by the loss cone instability, and also show that the saturation amplitude for the extraordinary mode increases in proportion to the ratio between electron cyclotron frequency and electron plasma frequency, in agreement with previous results obtained with numerical simulations. © *1997 American Institute of Physics.* [S1070-664X(97)04407-8]

I. INTRODUCTION

In natural plasmas and in laboratory experiments instabilities may be driven by inversion of the electron population in the direction perpendicular to the ambient magnetic field. For instance, this kind of instability is present in laboratory microwave generation devices,[1,2] and it is believed that it is also responsible for the phenomenon known as the Earth's kilometric radiation.[3–25] It has also been conjectured that the same class of instabilities can be found in a variety of other situations, such as in astrophysical radio sources,[26–28] planetary radio emissions,[29–32] and solar microwave bursts.[33–37] The theoretical analysis of this kind of instability requires relativistic effects in the description of the wave-particle interaction, and the instability is therefore called the *relativistic electron cyclotron maser* in the literature.

The existing literature on the cyclotron maser instability has usually emphasized linear features of the instability. The discussions which incorporate nonlinear features have frequently employed numerical simulation methods.[10,11,20,22] Some attempts have been made, however, to study the nonlinear stage of the instability by the use of quasilinear theory.[34–36,4,21,23] Among these attempts, particularly interesting for the present investigation is the work developed in Refs. 35 and 36, in which the set of fully self-consistent quasilinear particle and wave kinetic equations has been numerically solved, using the cold plasma dispersion relation and assuming that the cold electrons support the waves while the energetic population contributes to the growth of the waves.

Another recent investigation about the quasilinear evolution of the cyclotron maser instability, which also assumed that the instability is driven by a tenuous population of energetic electrons while a cold background plasma supports the wave motion, has been developed in Ref. 38. The approach utilized in Ref. 38 makes use of a model time-dependent distribution function and employs moments of the quasilinear equation, in order to obtain the time evolution of parameters of the distribution. The method has been employed for the study of a region of parameters for which the competition between different wave modes may be very important, and the conclusion has been that the mode with larger initial growth rate does not necessarily prevail over modes with smaller initial growth rates, in the late stage of the time evolution.[38]

The moment method has also been employed in another investigation, which fully incorporated thermal effects as well as the effect of the energetic electrons in the dispersion relation.[39] The method has been applied for parameters typical of the Earth's auroral zone, for a situation in which the relevant unstable modes are the fundamental extraordinary and ordinary modes. The results indicate that in the case of higher population of energetic electrons the fast diffusion saturates early the instability, at a wave level which is not very different from the level attained in the case of smaller population of energetic electrons.

For the present investigation on the quasilinear evolution of the electron cyclotron maser instability, however, we develop a formulation which does not make use of the moment method, deriving instead a quasilinear equation which can be numerically solved for the time evolution of the electron distribution function, self-consistently with the spectra of unstable waves. Both resonant and non-resonant diffusion are incorporated to the quasilinear equation. The formalism utilizes a dispersion relation in which thermal effects are fully taken into account, including the contribution of both the background electronic population and the population of energetic electrons (it has been demonstrated that these thermal effects can be important for the case of extraordinary mode waves with frequency near the electron cyclotron frequency[6]). For the numerical application of the formulation, we choose parameters motivated by the so-called auroral kilometric radiation (AKR). As it is known, this radiation phenomenon was first observed in the late 1960s and early 1970s,[40] and was successfully explained in terms of the weakly relativistic maser instability by Wu and Lee,[3] which identified the source of the instability as the loss-cone electrons that are formed when the energetic electrons injected

a)Electronic mail: ziebell@if.ufrgs.br

from the geomagnetic tail region are reflected by the converging geomagnetic field. We therefore assume a low-temperature background electron component along with a more energetic loss-cone population, and use a model loss-cone distribution as the initial state of the energetic electrons, along with a time-varying wave spectra in the unstable range of frequencies.

The organization of this paper is the following. In Sec. II we introduce the model electron distribution functions utilized as starting conditions for the time evolution, outline the derivation of the quasilinear equation and present a brief discussion on the dispersion relation for electromagnetic waves and on the procedure for obtaining the growth rate of the unstable waves. In Sec. III we briefly describe the method employed for the numerical solution of the quasilinear equation, and present the results of a numerical analysis, made for parameters typical of the auroral zones of the Earth. Finally, Sec. IV summarizes and discusses the results.

II. GENERAL FORMULATION

We are interested in instabilities that operate in the vicinity of the electron cyclotron frequency and/or its harmonics. Due to the high frequency nature of the waves, the ion response to any perturbation can be ignored, and therefore the ions only provide for charge neutrality. The electrons are assumed to feature a relatively cold component with density n_b and an energetic component with density n_h, possessing a one-sided loss-cone structure in momentum space. The geometry is such that the ambient magnetic field lies along the z direction ($\mathbf{B}_0=B_0\mathbf{e}_z$), with the wave vector $\mathbf{k}$ situated in the $x-z$ plane, $\mathbf{k}=k\ \sin\theta\,\mathbf{e}_x+k\ \cos\theta\,\mathbf{e}_z$.

A. Initial electron loss-cone distribution

The cold background population is represented by a low temperature Maxwellian distribution function

$$f_b(u,\mu)=\frac{1}{\pi^{3/2}\alpha_b^3}\ \exp\left(-\frac{u^2}{\alpha_b^2}\right), \tag{1}$$

where $\alpha_b^2=2T_b/m_ec^2$, with T_b being the temperature of the background electrons measured in energy units and m_e the electron mass. This background distribution is assumed to remain stationary along the time evolution of the system.

As the initial distribution function for the energetic electrons we assume the following model distribution function:[38]

$$f_h(u,\mu,t=0)=\frac{1}{\pi^{3/2}\alpha^3(0)}\ \exp\left(-\frac{u^2}{\alpha^2(0)}\right)G(\mu), \tag{2}$$

where

$$G(\mu)=\frac{1}{1-\delta\ \tanh(1/\delta)}\left[\tanh^2\left(\frac{\mu-1}{2\delta}\right)\right].$$

The parameter δ is related to the loss-cone angle $\theta_{\rm LC}$, according to the following expression:[39]

$$\theta_{\rm LC}=\cos^{-1}[1+\delta\ln(2-\sqrt{3})]. \tag{3}$$

The total thermal energy associated with the energetic loss-cone electrons is given by $E/m_ec^2=n_h\langle u^2/2\rangle=3n_h\alpha^2/4$, where $\langle\ldots\rangle=2\pi\int_{-1}^{1}d\mu\int_0^\infty du\ u^2\ldots f(u,\mu)$. Using the relation $E=3n_hT_h/2$ the effective temperature of the loss-cone electrons can be related to the parameter α as $T_h=m_ec^2\alpha^2/2$. Of course, $\alpha(0)$ appearing in Eq. (2) is the initial value of the quantity α. The variables u and μ appearing in Eqs. (1) and (2) are, respectively, the absolute value of the normalized momentum $\mathbf{u}=\mathbf{p}/(m_ec)$ and the cosine of the pitch angle.

B. Quasilinear formalism

We have assumed stationary background distribution. However, the energetic electron distribution may evolve in time. If the wave level is sufficiently small, this evolution may be described by the quasilinear approach. Following a standard textbook procedure, it is possible to arrive to the following expression for the quasilinear kinetic equation for the energetic electron component:

$$\partial_\tau f_h=\frac{1}{u^2}\partial_u\left\{(1-\mu^2)\left[u^2\left(D_{uu}\partial_u f_h-\frac{1}{u}D_{u\mu}\partial_\mu f_h\right)\right]\right\}-\frac{1}{u}\partial_\mu\left\{(1-\mu^2)\left[D_{\mu u}\partial_u f_h-\frac{1}{u}D_{\mu\mu}\partial_\mu f_h\right]\right\}, \tag{4}$$

where

$$D_{ab}=2\pi^2|\Omega_e|\sum_{n=-\infty}^{\infty}\int_{-\infty}^{\infty}dq\int_0^\infty dw\left|\frac{\tilde{E}_{wq}}{B_0}\right|^2|\hat{\mathbf{a}}_\mathbf{k}\cdot\mathbf{\Pi}_n|^2\times\frac{\gamma}{|\omega|}\delta(\gamma-nY-N_\parallel u\mu)\Delta_a\Delta_b,$$

$$\Delta_u=1,\Delta_\mu=\mu-\frac{N_\parallel u}{\gamma},$$

and where summation over unstable modes is implicit.[39] The quantity τ is the normalized time $\tau\equiv|\Omega_e|t$, $N_\parallel$ is the parallel component of $\mathbf{N}=c\mathbf{k}/\omega$, Ω_e is the electron cyclotron frequency, and $Y=|\Omega_e|/\omega$. Some details of the derivation of Eq. (4) appear in the Appendix, including the expression for $|\hat{\mathbf{a}}_\mathbf{k}\cdot\mathbf{\Pi}_n|^2$ in terms of the components of the dielectric tensor.

In Eq. (4) the spectral wave energy density has been expressed as a function of the normalized quantities $q\equiv ck_\parallel/|\Omega_e|$ and $w\equiv\omega/|\Omega_e|$. The spectral density is a time dependent quantity, which evolves in time according to

$$\frac{d}{d\tau}|\tilde{E}_{wq}|^2=2w_i|\tilde{E}_{wq}|^2, \tag{5}$$

where the normalized growth rate $w_i=\mathrm{Im}(w)$ can be self-consistently obtained from the dispersion relation. The perpendicular component of the wave vector ($N_\perp$), appearing in $|\hat{\mathbf{a}}_\mathbf{k}\cdot\mathbf{\Pi}_n|^2$, can also be obtained from the dispersion relation as a function of $N_\parallel$ and w, with $N_\parallel$ given by $N_\parallel=q/w$.

In the derivation leading to Eq. (4) vanishing growth rates have been assumed, and therefore only the effect of

resonant diffusion remains operative in the quasilinear evolution. However, non-resonant diffusion can be introduced at this stage, by the following procedure:[41]

$$\pi\frac{\gamma}{|\omega|}\delta(\gamma-nY-N_\parallel u\mu)$$
$$=\pi\delta\left(\omega-\frac{n|\Omega_e|}{\gamma}-\frac{ck_\parallel u_\parallel}{\gamma}\right)$$
$$=\lim_{\omega_i\to 0^+}\frac{\omega_i}{\left(\omega-\frac{n|\Omega_e|}{\gamma}-\frac{ck_\parallel u_\parallel}{\gamma}\right)^2+\omega_i^2}$$
$$=\lim_{w_i\to 0^+}\frac{1}{|\Omega_e|}\frac{w_i}{\left(w-\frac{n}{\gamma}-\frac{qu_\parallel}{\gamma}\right)^2+w_i^2}.$$

Therefore, considering that for the unstable waves the growth rates are small but finite, the components of the diffusion tensor appearing in Eq. (4) can be written as follows:

$$D_{ab}\simeq 2\pi\sum_{n=-\infty}^{\infty}\int_{-\infty}^{\infty}dq\int_0^\infty dw\left|\frac{\tilde{E}_{wq}}{B_0}\right|^2|\hat{\mathbf{a}}_\mathbf{k}\cdot\mathbf{\Pi}_n|^2$$
$$\times\frac{w_i}{\left(w-\frac{n}{\gamma}-\frac{qu_\parallel}{\gamma}\right)^2+w_i^2}\Delta_a\Delta_b. \tag{6}$$

Moreover, for small growth rate, it is possible to approximate $D_{ab}\simeq D_{ab}^r$ in the resonant region, where

$$D_{ab}^r=2\pi^2\sum_{n=-\infty}^{\infty}\int_{-\infty}^{\infty}dq\int_0^\infty dw\left|\frac{\tilde{E}_{wq}}{B_0}\right|^2|\hat{\mathbf{a}}_\mathbf{k}\cdot\mathbf{\Pi}_n|^2$$
$$\times\frac{\gamma}{|w|}\delta(\gamma-nY-N_\parallel u\mu)\Delta_a\Delta_b. \tag{7}$$

On the other hand, for $(w-n/\gamma-qu_\parallel/\gamma)^2\gg w_i^2$, the imaginary part of w can be neglected in the denominator and the non-resonant contribution to the diffusion tensor is obtained,

$$D_{ab}^{nr}=2\pi\sum_{n=-\infty}^{\infty}\int_{-\infty}^{\infty}dq\int_0^\infty dw\left|\frac{\tilde{E}_{wq}}{B_0}\right|^2|\hat{\mathbf{a}}_\mathbf{k}\cdot\mathbf{\Pi}_n|^2$$
$$\times\frac{w_i}{(w-n)^2}\Delta_a\Delta_b, \tag{8}$$

where we have further approximated $(w-(n/\gamma)-(qu_\parallel/\gamma))^2\simeq(w-n)^2$.

C. Dispersion relation

The dispersion relation is written as

$$\Lambda(\mathbf{k},\omega)=AN_\perp^4+BN_\perp^2+C=0, \tag{9}$$

where A, B and C are coeficients depending of the components of the dielectric tensor and on $N_\parallel$. Explicit expressions for A, B and C can be found in Ref. 39 and will not be repeated here. The components of the dielectric tensor are denoted as ε_{ij}, and can be written as follows:

$$\varepsilon_{ij}=\delta_{ij}+\delta_{i3}\delta_{j3}e_{33}+N_\perp^{\delta_{i3}+\delta_{j3}}\chi_{ij}, \tag{10}$$

where

$$e_{33}=\sum_\alpha X_\alpha\int d^3u\frac{u_\parallel\partial f_\alpha/\partial u_\parallel}{\gamma-N_\parallel u_\parallel},$$
$$\chi_{ij}=\sum_\alpha\frac{X_\alpha}{Y^{\delta_{i3}+\delta_{j3}}}\sum_{m=1}^{\infty}\left(\frac{N_\perp}{Y}\right)^{2(m-1)}$$
$$\times\sum_{n=-m}^{m}s_{ij}(n,m)I_\alpha(n,m,\delta_{i3}+\delta_{j3}),$$

and where the summation over α is over electron species. For these expressions, we have defined

$$I_\alpha(n,m,l)=\int d^3u\frac{u_\parallel^l u_\perp^{2m-1}}{\gamma-nY-N_\parallel u_\parallel}\frac{1}{\gamma}[(\gamma-N_\parallel u_\parallel)\partial_{u_\perp}$$
$$+N_\parallel u_\perp\partial_{u_\parallel}]f_\alpha,$$

and $X_\alpha=\omega_{p\alpha}^2/\omega^2$, where $\omega_{p\alpha}=(4\pi n_\alpha e^2/m_e)^{1/2}$ is the electron plasma frequency for species α [We define the total electron plasma frequency by $\omega_{pe}=(4\pi n_T e^2/m_e)^{1/2}$, where $n_T=\Sigma_\alpha n_\alpha$ is the total electron density.] The coefficients $s_{ij}(n,m)$ can also be found in Ref. 39 and will not be repeated here.

The $I_\alpha(n,m,l)$ integrals defined in Eq. (10) can be separated into real and imaginary parts, with the real part given by the principal part of the integral and the imaginary part being the contribution of the resonance $[I_\alpha(n,m,l)=I'_\alpha(n,m,l)+iI''_\alpha(n,m,l)]$. As it is known, the imaginary part $I''_\alpha(n,m,l)$ is very sensitive to features of the distribution function along the resonance curve in momentum space. The exact position of the resonance curve is very important for the correct description of wave particle resonance, and relativistic effects must be incorporated for the correct evaluation of the imaginary parts. Therefore, the modifications in the distribution function of energetic electrons which happen along the time evolution must be taken into account in the evaluation of the imaginary parts of I_α. In our formulation these integrals are evaluated numerically at each time step of the evolution, using the actual distribution function. Due to the azimuthal symmetry of the distribution function and to the delta function appearing in $I''_\alpha(n,m,l)$, only the $u_\parallel$ integral must be numerically performed.

On the other hand, the principal parts are dependent upon the integrated distribution and usually can be regarded as rather insensitive to detailed features in the distribution, unless some peculiar circumstances are satisfied.[42] This virtual independence on detailed features of the distribution justifies further approximations, which contribute very much to speeding up the quasilinear code. When evaluating the principal part of the integral $I_\alpha(n,m,l)$ for the energetic distribution we neglect the μ dependence of the distribution, thereby considering a Maxwellian distribution. Moreover, in order to avoid repeated evaluations, for the principal part we assume that the temperature of the distribution is constant along time evolution (a hypothesis which can be verified *a posteriori*, after application of the quasilinear procedure). These are the same hypotheses made in Ref. 39, and there-

fore the principal part of the integral $I_h(n,m,l)$ for the energetic population can be given by Eq. (19) of Ref. 39, and does not need to be repeated here. Similarly, the quantity e_{33} for the energetic particles can be given by Eq. (21) of Ref. 39.

For the case of the background distribution, which remains stationary throughout the time evolution, the same considerations can be made. Therefore, $I_b'(n,m,l)$ and e_{33} are given by the two Eqs. (22) of Ref. 39. The imaginary part $I_b''(n,m,l)$, which does not evolve in time, can be given by Eq. (23) of Ref. 39.

D. Derivation of the growth rates

The instantaneous growth rate, which is necessary for quasilinear evolution of the wave, is obtained from the solution of the dispersion relation. However, the dielectric tensor which appears in the coefficients of Eq. (9) exhibits a complex dependence on ω, when thermal effects are taken into account. As a consequence, the obtainment of the wave frequency as a function of $\mathbf{k}$, for a given mode, is not a trivial task, requiring sophisticated and time-consuming numerical procedures. In order to overcome this difficulty and to make the present quasilinear treatment tractable, we employ an approximate procedure, which turns out to be quite satisfactory as far as the frequency range in which significant growth occurs is not in the range of anomalous dispersion, and as far as the group velocity does not approach zero. The procedure has already been explained in Ref. 39, and will be only briefly exposed here.

We obtain the growth rate as follows. The dispersion relation as given by Eq. (9) is formally written as a quartic equation, with $N_\perp$ as the unknown. Therefore, the roots can be formally written as

$$N_\perp^2 = \frac{-B \pm \sqrt{B^2 - 4AC}}{2A}, \tag{11}$$

where the coefficients A, B, and C are in general functions of $N_\perp$.

An iterative procedure is applied to Eq. (11), starting with the evaluation of the cold plasma root corresponding to a specific mode, for a given value of the real wave frequency. The quantity $N_\parallel$ is treated as a parameter, since in the slab geometry the parallel component of the refraction index is constant along the trajectory of the radiation. Since away from the resonance the refraction index is real, the constancy of $N_\parallel$ along the ray in the proposed geometry assures that it is a real parameter.

The iterative procedure provides a complex value of $N_\perp$ (or $k_\perp$, since these quantities are proportional). For a finite group velocity, negative imaginary part of the wave vector implies that the wave amplitude grows convectively. Due to the finite group velocity, the growth along the ray path can be expressed equivalently as a temporal growth. This leads to an approximate expression for the growth rate,

$$\omega_i \simeq -k_i v_{gx}, \tag{12}$$

where v_{gx} is the x component of the group velocity, and k_i is the imaginary part of $k_\perp$.

III. NUMERICAL ANALYSIS AND RESULTS

Here the formalism developed in the previous section is applied to a situation typical of the auroral zones of the Earth. The parameters which are relevant for the application are the ratio of electron plasma to electron cyclotron frequency, $\eta \equiv \omega_{pe}/\Omega_e$, the ratio between the energetic electron density and the background electron density, $\rho \equiv n_h/n_b$, the background electron temperature T_b, and the initial values of the effective temperature of the energetic electrons, T_h, the loss cone angle, and the ratio between wave energy and particle energy.

In the auroral regions, it is recognized the existence of a population of hot electrons of magnetospheric origin, with effective temperature near 4 keV, which prevails over the cold population for $z \gtrsim 1.5\, R_E$, where R_E is the radius of the Earth, while the cold population dominates at low altitudes. It is also known that the ratio of plasma to cyclotron frequency is lower than $\eta = 0.1$ for $1.1\, R_E \lesssim z \lesssim 2\, R_E$, approaching $\eta = 1$ for $z \to 4\, R_E$, with recent observations emphasizing the occurrence of low density plasmas ($n_e < 1\ \mathrm{cm}^{-3}$) in the source region of the AKR.[43,44]

Taking these conditions into account, we do not assume any predominant electron population, using $\rho = 1$ in the application which follows. The background temperature is assumed to be $T_b = 0.2$ keV, the energetic temperature $T_h = 4$ keV, and the loss-cone angle is taken as $\theta_{\mathrm{LC}} = 30°$ (corresponding to $\delta = 0.1017304$). With these assumptions, we investigate the quasilinear evolution of the instability for low values of the parameter η, a situation which may be relevant for the AKR.

A. Numerical implementation of the quasilinear formalism

The solution of the dispersion relation for the initial conditions shows that the relevant modes are the fundamental X and O modes. The harmonics of these modes could be included in the analysis, in principle, but they are only weakly unstable when compared with the fundamental modes, and will therefore be neglected. The W mode is also stable, as well as the Z mode, which can play a very relevant role for higher density cases.[38]

We therefore proceed with the quasilinear evolution of the waves and the electron distribution function. We assume that the distribution of the spectral energy is uniform over the initially unstable region in (w,q) space, and vanishes outside of this region. The initial amplitude of the wave energy for each mode is determined by the initial value of the integrated spectrum, $E_{\mathrm{wave}}(0)$. Since only the fundamental X and O modes are relevant, they are the only modes included in the formulation. For the sake of simplicity, we assume the same initial level of wave energy for each mode, choosing the wave energy such that $E^X_{\mathrm{wave}}(0)/E_{\mathrm{particle}}(0) = E^O_{\mathrm{wave}}(0)/E_{\mathrm{particle}}(0) = 1.0 \times 10^{-4}$, where $E^X_{\mathrm{wave}}(0)/E_{\mathrm{particle}}(0)$ and $E^O_{\mathrm{wave}}(0)/E_{\mathrm{particle}}(0)$ are, respectively, the initial values of the ratio between wave energy in the X and O modes and particle energy associated with the energetic electrons,

$$\frac{E_{\text{wave}}}{E_{\text{particle}}}=\frac{\int d^3k(|\tilde{E}_{\mathbf{k}}|^2+|\tilde{B}_{\mathbf{k}}|^2)/(8\pi)}{n_h m_e c^2 \int d^3u(u^2/2)f_h}$$

$$=\frac{4\pi}{3\alpha^2}\left(1+\frac{n_b}{n_h}\right)\frac{\Omega_e^2}{\omega_{pe}^2}\int_{-\infty}^{\infty}dq\int_0^{\infty}dw\left|\frac{\tilde{E}_{wq}}{B_0}\right|^2$$

$$\times[1+|\mathbf{N}|^2(1-|\hat{\mathbf{a}}_{\mathbf{k}}\cdot\hat{\mathbf{k}}|^2)], \tag{13}$$

where $\hat{\mathbf{k}}$ is a unitary wave vector.

The time evolution proceeds by taking into account the unstable range of the wave field, for the evaluation of the diffusion coefficient utilized in the quasilinear equation, Eq. (4). The wave energy therefore increases while there is an unstable region in (w,q) space. Re-absorption of wave energy by the particles is not included in the analysis, and spontaneous emission has not been considered.

The equation for the time evolution of the distribution function is transformed into a set of finite difference equations in the (u,μ) space, using centered derivatives for the points inside the grid, and special equations using forward and backward μ derivatives at the extremes of the μ interval. We have considered a grid of 61×31 points in this space, for $0\leqslant u\leqslant u_{\text{lim}}$ (assuming $u_{\text{lim}}=0.5$), and for $-1\leqslant\mu\leqslant1$. Since for the unstable waves the wave-particle resonance occurs for small values of u, it is expected that the significant modifications of the distribution function will be restricted to this region, and therefore the distribution function is assumed to remain constant at $u=u_{\text{lim}}$. For the wave spectra, we have used a 31×31 grid in (w,q) space, concentrated in the region where the growth rates are significant. For the solution of the finite difference equations, we have used the method ADI (implicit in alternated directions), which leads to a tri-diagonal system of equations that can be solved by conventional methods.[45,46] In the dispersion relation we have neglected harmonics and utilized the small Larmor radius approximation.

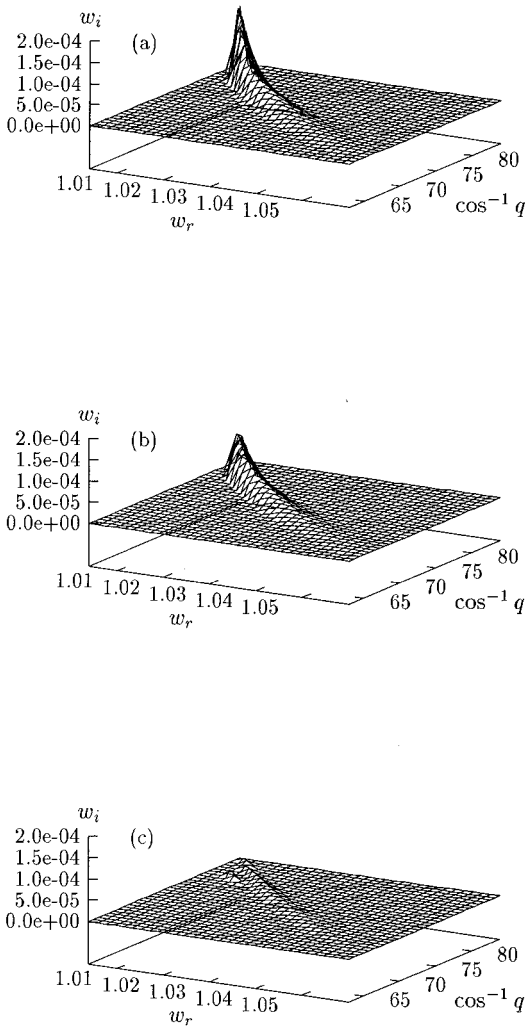

FIG. 1. Three-dimensional surface plots of the normalized growth rate for the X mode, for $\eta=0.01$. Parameters of the electron population: $\theta_{\text{LC}}=30°$, $T_h=4.0$ keV, $T_b=0.2$ keV; $E_{\text{wave}}(0)/E_{\text{particle}}=1.0\times10^{-4}$. (a) $\tau=0.$; (b) $\tau=2.0\times10^4$; (c) $\tau=5.0\times10^4$.

B. Results of the numerical analysis

We start the analysis by considering that both resonant and non-resonant diffusion are taking place. Although the values of the non-resonant diffusion coefficient are expected to be negligible when compared to the values of the resonant diffusion coefficient, non-resonant diffusion may be nevertheless effective, causing re-distribution of the particle population modified by the resonant interaction.

Initially we consider the case of $\eta=0.01$, and show in Figs. 1 and 2 the normalized growth rates for the X and O modes, versus normalized frequency w and $\cos^{-1}q$. The quantity $\cos^{-1}q$ approximately coincides with the propagation angle, for $w\simeq1$ and refractive index $\simeq1$, which is the case except near the cut-offs. The time step utilized in the calculation has been $\Delta\tau=500$. Considering the magnitude of the normalized growth rates, this value guarantees that the wave fields evolve very little in each time step, as required for the validity of the quasilinear treatment.

Figure 1(a) shows the initial values of the normalized growth rates for the X mode. It is seen that the absolute values of the growth rates are very small as compared to the values of the real frequencies, which is a requirement for the use of quasilinear theory. Figures 1(b) and 1(c) show, respectively, the normalized growth rates for the X mode at $\tau=2.0\times10^4$ and at $\tau=5.0\times10^4$. When comparing with the corresponding values at $\tau=0$ in Fig. 1(a), it is noticeable the reduction of the normalized growth rates, especially in the regions of $(w-q)$ space where they were more conspicuous at $\tau=0$. Similar considerations can be made about the O mode growth rates, appearing in Fig. 2.

The time evolution of the distribution function for magnetospheric electrons can be observed in Fig. 3, where we display three-dimensional surface plots of f_h, for the same case $\eta=0.01$. Panel (a) shows the initial distribution function, at $\tau=0$, and panel (b) shows the distribution function at $\tau=2.0\times10^4$. It is possible to see the partial filling of the loss-cone region, which continues and becomes more pronounced, as shown by panel (c) of Fig. 3, for $\tau=5.0\times10^4$. The evolution at this time is already quite slow, and the partial filling of the loss-cone region remains visually almost unchanged for larger values of τ. These results show that the

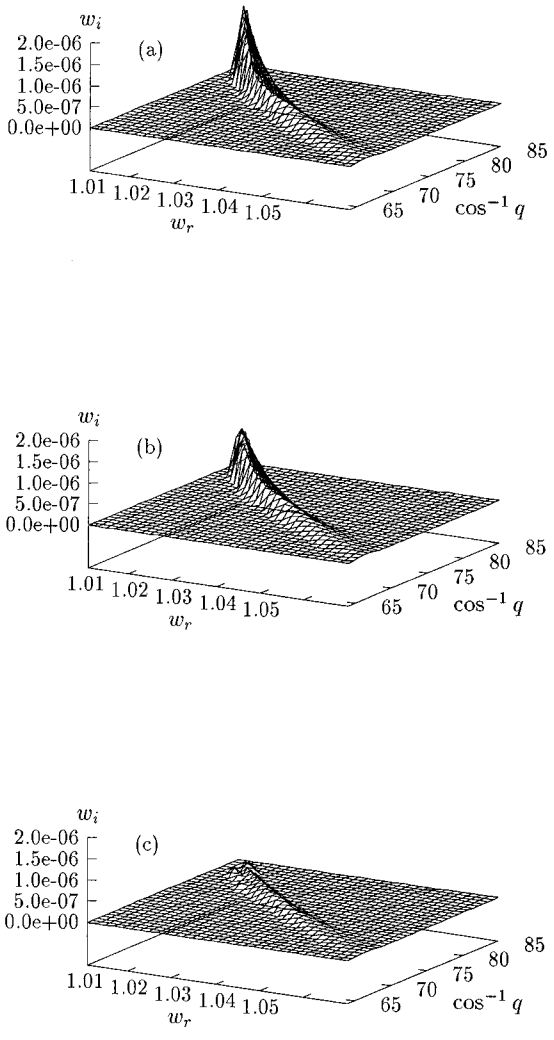

FIG. 2. Three-dimensional surface plots of the normalized growth rate for the O mode, for $\eta=0.01$. Parameters of the electron population: $\theta_{LC}=30°$, $T_h=4.0$ keV, $T_b=0.2$ keV; $E_{wave}(0)/E_{particle}=1.0\times10^{-4}$. (a) $\tau=0.$; (b) $\tau=2.0\times10^4$; (c) $\tau=5.0\times10^4$.

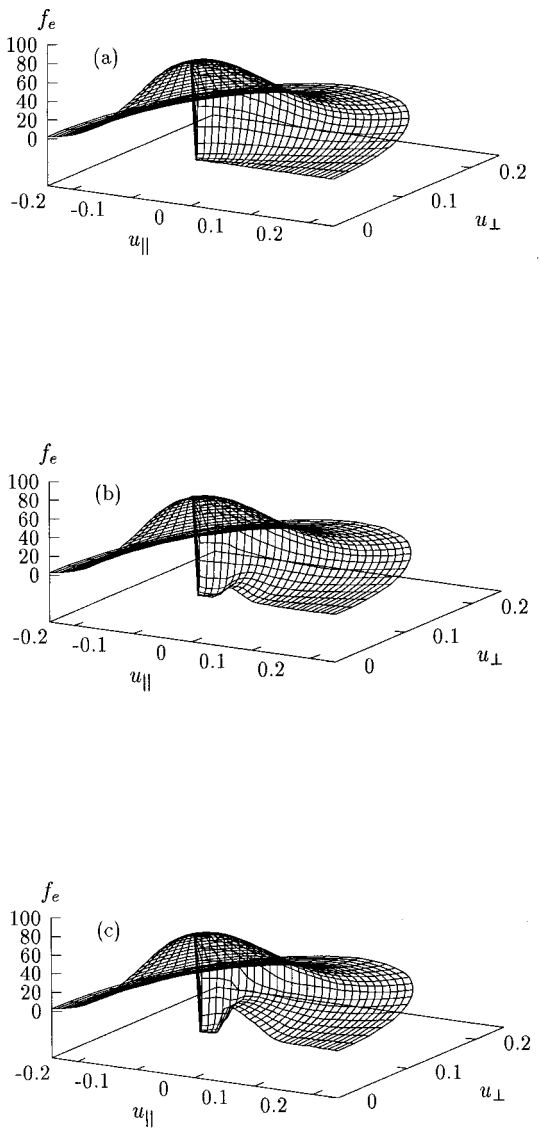

FIG. 3. Three-dimensional surface plots of the model distribution function for energetic electrons, for $\eta=0.01$ and other parameters as in Fig. 1. (a) $\tau=0.0$; (b) $\tau=2.0\times10^4$; (c) $\tau=5.0\times10^4$.

distribution function stabilizes asymptotically with a remaining degree of anisotropy which does not disappear due to the maser instability. The ''hole'' appearing for small values of u is not really a hole in the total distribution function, since it is filled up by the low temperature background particles.

The modification of the distribution function can be seen from a different point of view in Fig. 4, in which we show the evolution of the parameter $\alpha(\tau)$ as a function of normalized time τ, for three values of η ($\eta=0.01$, 0.03, and 0.05). For $\eta=0.03$ and 0.05 the time steps utilized have been $\Delta\tau=167$ and $\Delta\tau=100$, respectively. This parameter α is related to the energy content of the energetic distribution function (E is proportional to α^2), and the result indicates the relatively small decrease in the energy content of the magnetospheric electron distribution, due to the maser instability, for the three cases considered. The small decrease in the temperature of the energetic electrons justifies the assumption of constant temperature, made for the evaluation of the Hermitian part of the dielectric tensor.

The time evolution of $E_{wave}/E_{particle}(0)$ is displayed in Fig. 5. Panel (a) shows the case of the X mode, and panel (b) the case of the O mode. The asymptotic value of $E_{wave}/E_{particle}(0)$ for the X mode appears to be nearly pro-

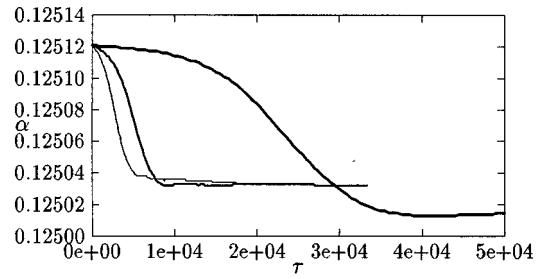

FIG. 4. Time evolution of the parameter $\alpha(\tau)$, for three values of η and other parameters as in Fig. 1. Bold line, $\eta=0.01$; normal line, $\eta=0.03$; thin line, $\eta=0.05$.

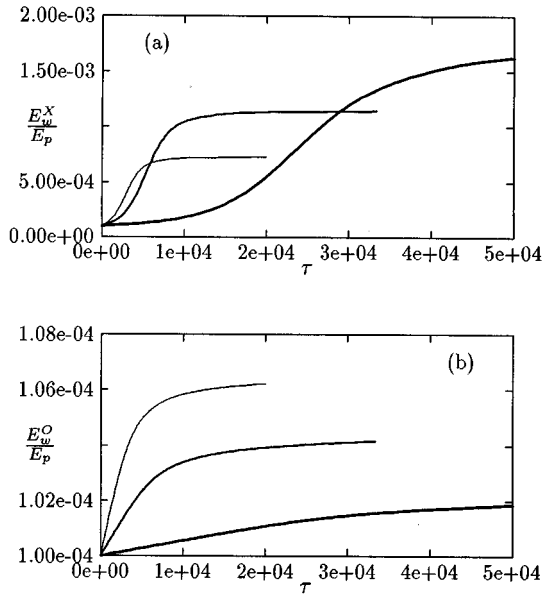

FIG. 5. Time evolution of $E_{\text{wave}}/E_{\text{particle}}$, for three values of η and other parameters as in Fig. 1. Bold line, $\eta=0.01$; normal line, $\eta=0.03$; thin line, $\eta=0.05$. (a) X mode; (b) O mode.

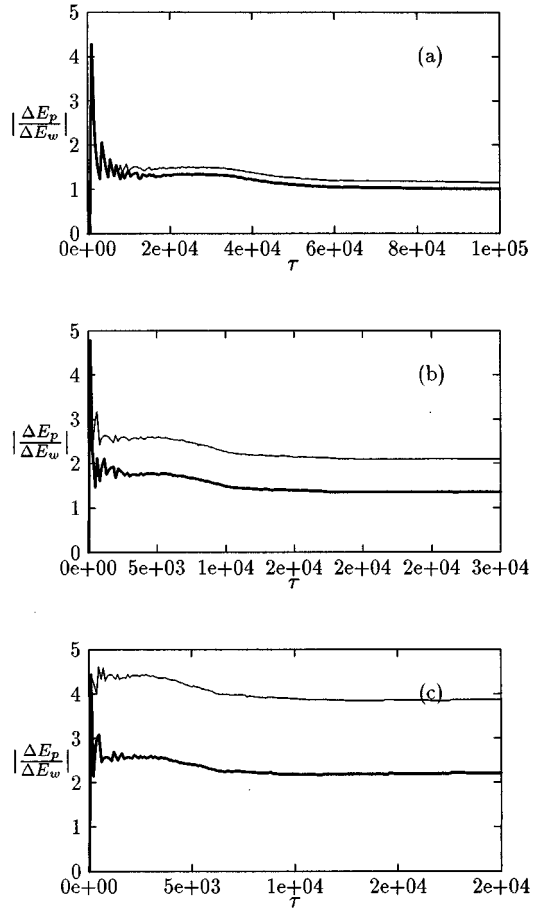

FIG. 6. Time evolution of the parameter $|\Delta E_p/\Delta E_w|$, for three values of η and other parameters as in Fig. 1. Bold line, calculation including non-resonant diffusion; thin line, calculation without non-resonant diffusion.

portional to Ω_e/ω_e, similarly to what has been obtained with numerical simulations conducted in the same range of electron energies[21]. The growth of the O mode waves has been negligible, as indicated by panel (b) of Fig. 5.

These results indicate that the evolution is qualitatively similar in the whole range of values of η considered in the present application. The quantitative difference is the saturation level of the wave energy, which increases with the decrease of η, and the time scale for the evolution. The diffusion time is larger for smaller η, due to the smaller growth rates. The amplitude of the wave field therefore grows at a slower pace, and the ensuing slow diffusion keeps the waves growing longer time than in the case of large η. For the parameters considered, only $0.1\%\sim0.2\%$ of the particle energy is finally converted into wave energy by the instability, an efficiency similar to that obtained with another quasilinear approach using a cold plasma dispersion relation.[35]

At this point it is useful to comment upon some of the properties of the code utilized. As it is well known, quasilinear theory conserves the number of particles, as well as momentum and energy of the wave-particle system. However, some approximations have been introduced in the present quasilinear approach, and it is useful to analyze the outcome of the calculations.

For instance, considering the case of $\eta=0.05$, we have tested the code and verified that the normalization of the distribution decreases by a factor $\simeq 1.5\times10^{-3}$, for τ between 0 and 1.0×10^4. This small decrease could be nonetheless relevant for the energy content of the distribution, since the efficiency of energy conversion is expected to be less than 1% of the total particle energy. Therefore, we introduced a renormalization of the distribution function at each time step, which assures the property of conservation of number of particles, as required by quasilinear theory. The results presented in this section have been obtained using this renormalization along the time evolution.

As far as energy conservation is concerned, we have obtained results which are qualitatively consistent but quantitatively sensitive to small changes in the parameters of the numerical solution, due to the very small relative modification in particle energy (less than 1%). The loss of energy by the particles may be evaluated from the initial and present values of α

$$\Delta E_{\text{particle}}=(\alpha^2/\alpha_0^2-1)E_{\text{particle}}(0),$$

while the increase in the wave energy comes directly from the addition of the X and O contributions as given by Fig. 5, at each value of τ.

In Fig. 6 we plot the quantity $|\Delta E_p/\Delta E_w|$, for $\eta=0.01$, 0.03, and 0.05, where the indexes p and w stand for ''particle'' and ''wave,'' respectively. The case of $\eta=0.01$ is shown in Fig. 6(a), where the bold line indicates the result obtained when non-resonant diffusion is taken into account along the quasilinear evolution. It is seen that, after a transient phase, the quantity $|\Delta E_p/\Delta E_w|$ stabilizes very near unity, indicating good properties of energy conservation. If the calculation is made for the same parameters without taking into account the non-resonant diffusion, we obtain the result denoted by the thin line in Fig. 6(a). This result is

qualitatively similar to that obtained with non-resonant diffusion, but stabilizes around $|\Delta E_p/\Delta E_w| \simeq 1.15$, indicating worst energy conservation.

For other values of η the time evolution is similar, as shown by Figs. 6(b) and 6(c) for $\eta = 0.03$ and $\eta = 0.05$, respectively. It can be seen that the asymptotic value of the ratio $|\Delta E_p/\Delta E_w|$ is progressively more distant from unity. It can also be seen that this ratio is larger when non-resonant diffusion is not taken into account in the quasilinear equation. Therefore, the results shown in Fig. 6 indicate that the approximations introduced in the present treatment, either analytically or numerically, are progressively less adequate as the parameter η is increased. However, although the energy conservation feature of the code becomes very poor for increasing η, other features of the quasilinear evolution are similar to those obtained in the case of small η, and therefore the results obtained in the whole range of η can be regarded at least as qualitative indications upon the actual behaviour of the solution.

One of the qualitative features which emerge from the results obtained is indeed the effect of non-resonant diffusion. The results show that the energy conservation is more strongly violated when non-resonant diffusion is neglected than when it is taken into account, specially for larger values of η (when the growth rates are larger). The comparison between the asymptotic values indicated by the bold lines and the thin lines in Fig. 6 indicates that a significant part of the energy lost by resonant particles is not really going into wave growth but is redistributed among the particles by non-resonant diffusion. This redistribution of energy by non-resonant diffusion has already been recognized in simpler situations, as in the textbook case of the ''bump-in-tail'' instability,[41] but it is usually not taken into account in quasilinear calculations.

Finally, it is interesting to compare the asymptotic distribution function obtained for the energetic electrons with the distribution obtained in a quasilinear analysis using moments of the quasilinear equation.[38,39] As expected, some features of the quasilinear evolution obtained with the simplified moment approach are qualitatively similar to those obtained with the present full numerical solution, but interesting details of the evolution of the distribution function are described here which can not be observed with the simplified approach. The difference is visually observable in the shape of the asymptotic distribution function, in three-dimensional (3D) plots like those of Fig. 3. The anysotropy depicted in Fig. 3(c) is different from the residual anisotropy which can be seen in Fig. 1(c) of Ref. 39, for instance. There are also other quantitative differences in the results, like the smaller efficiency of the energy diffusion and the smaller growth of the wave field obtained with the present approach, when compared with the previous moment method (as in the case with $\eta = 0.05$ and $\rho = 1$, in Ref. 39). Another important difference is that the time scale for saturation appears to be much faster in the present full numerical approach than obtained in the case of the moment method.[39]

IV. SUMMARY AND CONCLUSIONS

In the present paper we have carried out a quasilinear analysis of the electron cyclotron maser instability driven by a loss-cone population, introducing thermal effects and using the full dispersion relation in the quasilinear treatment of the loss-cone instability. As an application of the formalism, we have chosen a set of parameters typical of the Earth's auroral zone plasma, which may be relevant to the description of the auroral kilometric radiation. For the parameters chosen, the ratio between electron plasma frequency and electron cyclotron frequency is sufficiently small in order that the only relevant unstable modes are the fundamental X and O modes. In the present investigation, we did not conduct a general numerical investigation of the effect of the many parameters involved, prefering instead a single example as illustration of the use of the formalism. In general, it is not possible to foresee the effect of a given parameter. For instance, a parameter which certainly is significant for the growth rate and the saturation level of the instability is the loss-cone angle. However, there are many features to be considered. On one hand, smaller loss-cone angles are easier to fill-up, which could imply faster saturation of the quasilinear process. On the other hand, smaller loss-cone angles feature sharper gradients in velocity space, which may imply larger initial growth rates in some frequency range, and therefore faster wave growth. Therefore, only a careful investigation can display the actual dependence on this parameter.

In addition to the parameters, there are other potentially interesting features involved. For instance, different forms of the initial distribution function, while conserving the loss-cone character, may give rise to different initial growth rates and possibly non-trivially modify the outcome of the calculation. We intend to investigate these non-trivial features in the near future, and report any interesting findings in a forthcoming publication.

The numerical analysis of the self-consistent set of equations governing the evolution of the particle distributions and the wave fields, for the case considered, demonstrated that only $0.1\% \sim 0.2\%$ of the particle energy is converted to wave energy by the loss-cone instability. The dependence of the amplification efficiency on the frequency ratio ω_{pe}/Ω_e has been briefly discussed, and it has been seen that the saturation amplitude for X mode waves increases when this frequency ratio is decreased, in agreement with results previously obtained by means of numerical simulations. Of course, the agreement in this feature does not mean complete equivalence between the present quasilinear results and results obtained by numerical simulations. Numerical simulations, as well as quasilinear simulations, can be made with a variety of constraints and assumptions, and detailed comparisons are usually difficult and not conclusive.

The formalism and the numerical analysis utilized incorporated both resonant and non-resonant diffusion in the quasilinear equation for the particle distribution. The numerical results have indicated that the effect of non-resonant diffusion is significant and increases with the increase of the ratio ω_{pe}/Ω_e, due to the larger growth rates. Although the results regarding energy conservation are only qualitative, the indication is that a considerable fraction of the energy involved

in wave-particle resonance processes is not converted into wave energy, being only redistributed among the particles by non-resonant diffusion. When non-resonant diffusion is not considered, this fraction of energy simply disappears from the system and the energy conservation properties of the numerical solution considerably degrade.

The comparison between the results of the present full numerical approach and the results obtained in previous studies which utilized a moment method for the time evolution of the distribution function indicates that the moment method super estimates the efficiency of energy conversion and predicts larger wave amplification than the full numerical method, for the same parameters. The time scale for saturation predicted by the full numerical approach is considerably shorter than predicted by the moment method. The distribution functions found with the use of these two approaches feature some differences visually perceptible in 3D plots, although both methods predict that the asymptotic state of the instability is attained with partial filling up of the loss-cone, with certain degree of pitch angle anisotropy remaining in the distribution function.

ACKNOWLEDGMENTS

This work has been partially supported by the Brazilian agencies Conselho Nacional de Desenvolvimento Científico e Tecnológico (CNPq) and Financiadora de Estudos e Projetos (FINEP). Numerical computations were performed at the Supercomputer Center installed at the Universidade Federal do Rio Grande do Sul (CESUP-UFRGS).

APPENDIX: SUMMARY OF THE DERIVATION OF THE QUASILINEAR EQUATION

The quasilinear kinetic equation for the energetic electron component may be derived with the use of a standard textbook procedure, resulting

$$\partial_t f_e=\frac{1}{u_\perp}L'\left[\frac{u_\perp}{\gamma}\frac{\pi e^2}{m_e^2c^2}\sum_{n=-\infty}^{\infty}\int d^3k|\tilde{E}_{\mathbf{k}}|^2|\hat{\mathbf{a}}_{\mathbf{k}}\cdot\mathbf{\Pi}_n|^2 \times\frac{1}{\gamma}(Lf_e)\frac{\gamma}{|\omega|}\delta(\gamma-nY-N_\parallel u_\parallel)\right], \tag{A1}$$

where summation over unstable modes is implicit, $\hat{\mathbf{a}}_{\mathbf{k}}$ is the polarization vector, L and L' are differential operators respectively given by $L=nY\partial_{u_\perp}+N_\parallel u_\perp\partial_{u_\parallel}$ and $L'=nY\partial_{u_\perp}+u_\perp\partial_{u_\parallel}N_\parallel$, and

$$\begin{aligned}\hat{\mathbf{a}}_{\mathbf{k}}\cdot\mathbf{\Pi}=(-1)^n\{&[\varepsilon_{12}(\varepsilon_{33}-N_\perp^2)+\varepsilon_{23}(\varepsilon_{13}+N_\parallel N_\perp)]\Pi_1^n\\&+[(\varepsilon_{13}+N_\parallel N_\perp)^2-(\varepsilon_{11}-N_\parallel^2)(\varepsilon_{33}-N_\perp^2)]\Pi_2^n\\&-[\varepsilon_{23}(\varepsilon_{11}-N_\parallel^2)+\varepsilon_{12}(\varepsilon_{13}+N_\perp N_\parallel)]\Pi_3^n\}\\&\times\{-[\varepsilon_{12}(\varepsilon_{33}-N_\perp^2)+\varepsilon_{23}(\varepsilon_{13}+N_\perp N_\parallel)]^2\\&+[(\varepsilon_{13}+N_\parallel N_\perp)^2-(\varepsilon_{11}-N_\parallel^2)(\varepsilon_{33}-N_\perp^2)]^2\\&-[\varepsilon_{23}(\varepsilon_{11}-N_\parallel^2)+\varepsilon_{12}(\varepsilon_{13}+N_\perp N_\parallel)]^2\}^{-1/2}.\end{aligned}$$

The ε_{ij} are the components of the dielectric tensor, and the Π_i^n are given by

$$\Pi_1^n=-\frac{n}{\lambda}J_n(\lambda),\qquad \Pi_2^n=iJ_n'(\lambda),$$

$$\Pi_3^n=\frac{u_\parallel}{u_\perp}J_n(\lambda),\qquad \lambda=\frac{-N_\perp u_\perp}{Y},$$

where the J_n and J_n' are, respectively, the Bessel function of order n and its derivative, with $u_\parallel$ and $u_\perp$ being, respectively, the parallel and perpendicular components of the normalized particle momentum, $\mathbf{u}$.

Equation (A1) can be cast in more convenient form by defining auxiliary quantities,

$$\hat{D}_{ab}=\frac{\pi e^2}{m_e^2c^2}\sum_{n=-\infty}^{\infty}\int d^3k\left|\frac{\tilde{E}_{wq}}{B_0}\right|^2|\hat{\mathbf{a}}_{\mathbf{k}}\cdot\mathbf{\Pi}_n|^2\frac{\gamma}{|\omega|} \times\delta(\gamma-nY-N_\parallel u_\parallel)\hat{\Delta}_a\hat{\Delta}_b,$$

$$\hat{\Delta}_\perp=1-N_\parallel u_\parallel/\gamma,\qquad \hat{\Delta}_\parallel=N_\parallel u_\perp/\gamma,$$

resulting

$$\begin{aligned}\partial_t f_e=&\frac{1}{u_\perp}\partial_{u_\perp}[u_\perp(\hat{D}_{\perp\perp}\partial_{u_\perp}f_e+\hat{D}_{\perp\parallel}\partial_{u_\parallel}f_e)]\\&+\partial_{u_\parallel}[\hat{D}_{\parallel\perp}\partial_{u_\perp}f_e+\hat{D}_{\parallel\parallel}\partial_{u_\parallel}f_e].\end{aligned}\tag{A2}$$

Defining new variables $u\equiv(u_\perp^2+u_\parallel^2)^{1/2}$ and $\mu\equiv u_\parallel(u_\perp^2+u_\parallel^2)^{-1/2}$, and after some simple algebraic manipulation, we arrive to

$$\begin{aligned}\partial_\tau f_h=&\frac{1}{u^2}\partial_u\left\{u^2\left[\hat{D}_{uu}\partial_u f_h-\frac{(1-\mu^2)^{1/2}}{u}\hat{D}_{u\mu}\partial_\mu f_h\right]\right\}\\&-\frac{1}{u}\partial_\mu\left\{(1-\mu^2)^{1/2}\left[\hat{D}_{\mu u}\partial_u f_h\right.\right.\\&\left.\left.-\frac{(1-\mu^2)^{1/2}}{u}\hat{D}_{\mu\mu}\partial_\mu f_h\right]\right\}\end{aligned}\tag{A3}$$

where

$$\hat{D}_{uu}=(1-\mu^2)\hat{D}_{\perp\perp}+2\mu(1-\mu^2)^{1/2}\hat{D}_{\perp\parallel}+\mu^2\hat{D}_{\parallel\parallel},$$

$$\begin{aligned}\hat{D}_{u\mu}=\hat{D}_{\mu u}=&\mu(1-\mu^2)^{1/2}\hat{D}_{\perp\perp}-(1-2\mu^2)\hat{D}_{\perp\parallel}\\&+\mu(1-\mu^2)^{1/2}\hat{D}_{\parallel\parallel},\end{aligned}$$

$$\hat{D}_{\mu\mu}=\mu^2\hat{D}_{\perp\perp}-2\mu(1-\mu^2)^{1/2}\hat{D}_{\perp\parallel}+(1-\mu^2)\hat{D}_{\parallel\parallel}.$$

With the use of the definitions of $\hat{\Delta}_\perp$ and $\hat{\Delta}_\parallel$, given before Eq. (A2), and introducing the electron cyclotron frequency, it is easy to show that these expressions can be written as follows:

$$\hat{D}_{uu}=(1-\mu^2)\pi|\Omega_e|\sum_{n=-\infty}^{\infty}\int d^3k\left|\frac{\tilde{E}_{wq}}{B_0}\right|^2|\hat{\mathbf{a}}_{\mathbf{k}}\cdot\mathbf{\Pi}_n|^2 \times\frac{\gamma}{|\omega|}\delta(\gamma-nY-N_\parallel u\mu),$$

$$\hat{D}_{u\mu}=(1-\mu^2)^{1/2}\pi|\Omega_e|\sum_{n=-\infty}^{\infty}\int d^3k\left|\frac{\tilde{E}_{wq}}{B_0}\right|^2|\hat{\mathbf{a}}_{\mathbf{k}}\cdot\mathbf{\Pi}_n|^2$$

$$\times\frac{\gamma}{|\omega|}\delta(\gamma-nY-N_{\|}u\mu)(\mu-N_{\|}u/\gamma),$$

$$\hat{D}_{\mu\mu}=\pi|\Omega_e|\sum_{n=-\infty}^{\infty}\int d^3k\left|\frac{\tilde{E}_{wq}}{B_0}\right|^2|\hat{\mathbf{a}}_{\mathbf{k}}\cdot\mathbf{\Pi}_n|^2\frac{\gamma}{|\omega|}$$

$$\times\delta(\gamma-nY-N_{\|}u\mu)(\mu-N_{\|}u/\gamma)^2.$$

After using these expressions into Eq. (A3), and introducing the dimensionless variables $\tau=|\Omega_e|t$, $q\equiv ck_{\|}/|\Omega_e|$, and $w\equiv\omega/|\Omega_e|$, and expressing the spectral wave energy density as a function of these normalized quantities,

$$\int d^3k|\tilde{E}_{\mathbf{k}}|^2=2\pi\int_{-\infty}^{\infty}dq\int_0^{\infty}dw|\tilde{E}_{wq}|^2,$$

we arrive at the following:

$$\partial_\tau f_h=\frac{1}{u^2}\partial_u\left\{(1-\mu^2)\left[u^2\left(D_{uu}\partial_u f_h-\frac{1}{u}D_{u\mu}\partial_\mu f_h\right)\right]\right\}$$

$$-\frac{1}{u}\partial_\mu\left\{(1-\mu^2)\left[D_{\mu u}\partial_u f_h-\frac{1}{u}D_{\mu\mu}\partial_\mu f_h\right]\right\},\quad\text{(A4)}$$

where we have defined

$$D_{ab}=2\pi^2|\Omega_e|\sum_{n=-\infty}^{\infty}\int_{-\infty}^{\infty}dq\int_0^{\infty}dw\left|\frac{\tilde{E}_{wq}}{B_0}\right|^2|\hat{\mathbf{a}}_{\mathbf{k}}\cdot\mathbf{\Pi}_n|^2$$

$$\times\frac{\gamma}{|\omega|}\delta(\gamma-nY-N_{\|}u\mu)\Delta_a\Delta_b,$$

$$\Delta_u=1,\qquad\Delta_\mu=\mu-\frac{N_{\|}u}{\gamma}.$$

Equation (A4) is precisely Eq. (4), which appears is Sec. II giving the time evolution of the distribution function for the energetic electron component.

[1]H. S. Uhm, R. C. Davidson, and K. R. Chu, Phys. Fluids **21**, 1886 (1978).
[2]H. S. Uhm and R. C. Davidson, Phys. Fluids **29**, 2713 (1986).
[3]C. S. Wu and L. C. Lee, Astrophys. J. **230**, 621 (1979).
[4]C. S. Wu, S. T. Tsai, M. J. Xu, and J. W. Shen, Astrophys. J. **248**, 384 (1981).
[5]N. Omidi and D. A. Gurnett, J. Geophys. Res. **89**, 10801 (1984).
[6]H. K. Wong, C. S. Wu, F. J. Ke, R. S. Schneider, and L. F. Ziebell, J. Plasma Phys. **28**, 503 (1982).
[7]C. S. Wu, H. K. Wong, D. J. Gorney, and L. C. Lee, J. Geophys. Res. **87**, 4476 (1982).
[8]D. B. Melrose, K. G. Ronmark, and R. G. Hewitt, J. Geophys. Res. **87**, 5140 (1982).
[9]P. B. Dusenbery and L. R. Lyons, J. Geophys. Res. **88**, 10072 (1983).
[10]J. S. Wagner, L. C. Lee, C. S. Wu, and T. Tajima, Geophys. Res. Lett. **10**, 483 (1983).
[11]J. S. Wagner, L. C. Lee, C. S. Wu, and T. Tajima, Radio Sci. **19**, 509 (1984).
[12]C. S. Wu and X. M. Qiu, J. Geophys. Res. **89**, 883 (1984).
[13]N. Omidi, C. S. Wu, and D. A. Gurnett, J. Geophys. Res. **89**, 883 (1984).
[14]D. B. Melrose, R. G. Hewitt, and G. A. Dulk, J. Geophys. Res. **89**, 897 (1984).
[15]D. LeQuéau, R. Pellat, and A. Roux, J. Geophys. Res. **89**, 2831 (1984).
[16]D. LeQuéau, R. Pellat, and A. Roux, Phys. Fluids **27**, 247 (1984).
[17]D. LeQuéau and P. Louarn, J. Geophys. Res. **94**, 2605 (1989).
[18]C. S. Wu, Space Sci. Rev. **41**, 215 (1985).
[19]N. Omidi and C. S. Wu, J. Geophys. Res. **90**, 6641 (1985).
[20]P. L. Pritchett and R. J. Strangeway, J. Geophys. Res. **90**, 9650 (1985).
[21]P. L. Pritchett, Phys. Fluids **29**, 2919 (1986).
[22]P. L. Pritchett and R. M. Winglee, J. Geophys. Res. **94**, 129 (1989).
[23]P. H. Yoon and C. S. Wu, Phys. Rev. A **33**, 6819 (1991).
[24]R. Gaelzer, L. F. Ziebell, and R. S. Schneider, J. Geophys. Res. **97**, 19299 (1992).
[25]R. Gaelzer, L. F. Ziebell, and R. S. Schneider, J. Geophys. Res. **99**, 8905 (1994).
[26]D. E. Gary, J. L. Linsky, and G. A. Dulk, Astrophys. J. L **79**, 263 (1982).
[27]K. A. Lang and R. F. Wilson, Astrophys. J. **305**, 6423 (1986).
[28]P. H. Yoon and T. Chang, Astrophys. J. **343**, 31 (1989).
[29]P. Galopeau, P. Zarka, and D. L. Quéau, J. Geophys. Res. **94**, 8739 (1989).
[30]H. P. Ladreiter and Y. Leblanc, J. Geophys. Res. **95**, 367 (1990).
[31]S. A. Curtis, Nature (London) **318**, 47 (1985).
[32]Y. Leblanc, Adv. Space Res. **10**, 39 (1990).
[33]D. B. Melrose and G. Dulk, Astrophys. J. **259**, 844 (1982).
[34]M. J. Aschwanden and A. O. Benz, Astrophys. J. **332**, 447 (1988).
[35]M. J. Aschwanden, Astron. Astrophys. Suppl. Ser. **85**, 1141 (1990).
[36]M. J. Aschwanden, Astron. Astrophys. **237**, 512 (1990).
[37]M. Güdel, Astron. Astrophys. Lett. **1**, 239 (1990).
[38]P. H. Yoon and L. F. Ziebell, Phys. Rev. E **51**, 4908 (1995).
[39]L. F. Ziebell and P. H. Yoon, Phys. Plasmas **2**, 1285 (1995).
[40]D. A. Gurnett, J. Geophys. Res. **79**, 4227 (1974).
[41]R. C. Davidson, *Methods in Nonlinear Plasma Theory* (Academic, New York, 1972).
[42]L. F. Ziebell and G. Granata, Phys. Fluids **29**, 3730 (1986).
[43]P. Louarn, A. Roux, H. de Féraudy, D. LeQuéau, M. André, and L. Matson, J. Geophys. Res. **95**, 5983 (1990).
[44]A. Hilgers, B. Holback, G. Holmgren, and R. Boström, J. Geophys. Res. **97**, 8631 (1992).
[45]B. Carnahan, H. Luther, and J. Wilkes, *Applied Numerical Methods* (Wiley, New York, 1969).
[46]W. H. Press, B. P. Flannery, S. A. Teukolsky, and W. T. Vetterling, *Numerical Recipes—The Art of Scientific Computing* (Cambridge University Press, Cambridge, 1989).